

Accordo Attuativo ASI-INAF n. 2020-35-HH.0 per "Attività di studio della comunità nazionale dello Space Weather per il popolamento del prototipo di centro dati scientifico ASPIS"



**CAESAR - Comprehensive spAce wEather Studies for the ASPIS prototype Realization**

## SuperDARN data handling for NODE2000

WP1410

Prepared by	Iginò Coco		
Checked by	Maria Federica Marcucci, Stefano Massetti		
Approved by	Stefano Massetti		
Reference			
Issue	1	Revision	0
Date of issue			

Project Prime:

Project Partners:



# 1. Introduction

The current document is a technical pamphlet for the benefit of CAESAR NODE 2000 staff, in order to allow them to set up a representation of SuperDARN data in line with the standards of the SuperDARN community.

A short introduction will be given in Section 2 on what SuperDARN is, and what kind of SuperDARN data are currently distributed to the CAESAR NODE 2000. The actual format of data is detailed in Section 3. In Section 4 we will outline the procedure for representing the SuperDARN isocontours of electric potential in the polar cap starting from coefficients of a spherical harmonics expansion and finally, in Section 5, we will also give some considerations on the Altitude Adjusted and Corrected GeoMagnetic (AACGM) coordinate system, which is the preferred representation for SuperDARN data.

**A word of caution:** The data processing and representation within the SuperDARN community is automatically done by an open source software, the Radar Software Toolkit (RST, [1]). We neither usually need to go into the details of parameters computation starting from raw data, nor into the details of their representation on maps. This document constitutes an effort in explaining some basics of such matters, but let's be honest on the fact that our technical knowledge is limited and goes little further than what is described hereafter.

## 2. What is SuperDARN

The Super Dual Auroral Radar Network (SuperDARN) is an international network of High Frequency coherent scatter radars. A map of the fields of view of the radars currently in operation can be seen in Figure 1: INAF-IAPS manages the radar pair of Dome C East (DCE) and Dome C North (DCN) located at the Concordia station, in Antarctica, whose fields of view are shaded in green in the figure.

The SuperDARN concept is described in detail in [2]. A SuperDARN radar is a bistatic apparatus (i.e. the same antennae and the same electronics are used to both transmit and receive signals to/from the ionosphere), which works in the 8-20 MHz frequency range: coded sequences of radio pulses are steered through a field of view several tens degrees wide along a number of "beams" (directions), so that the whole field of view is covered in one or two minutes, depending on the operating mode. Along each beam, the pulse sequence defines from 75 to 100 range gates, from 180 km up to 3000 km from the radar site, where the radio signals encounter plasma density irregularities in the ionosphere, which cause such signals to be scattered back along the same direction. As ionospheric irregularities are dragged in the large scale convection at high latitudes,

the measure of the Doppler phase shift between the emitted and backscattered waves allows to infer the velocity of the ambient plasma with respect to the sounded direction and gate.

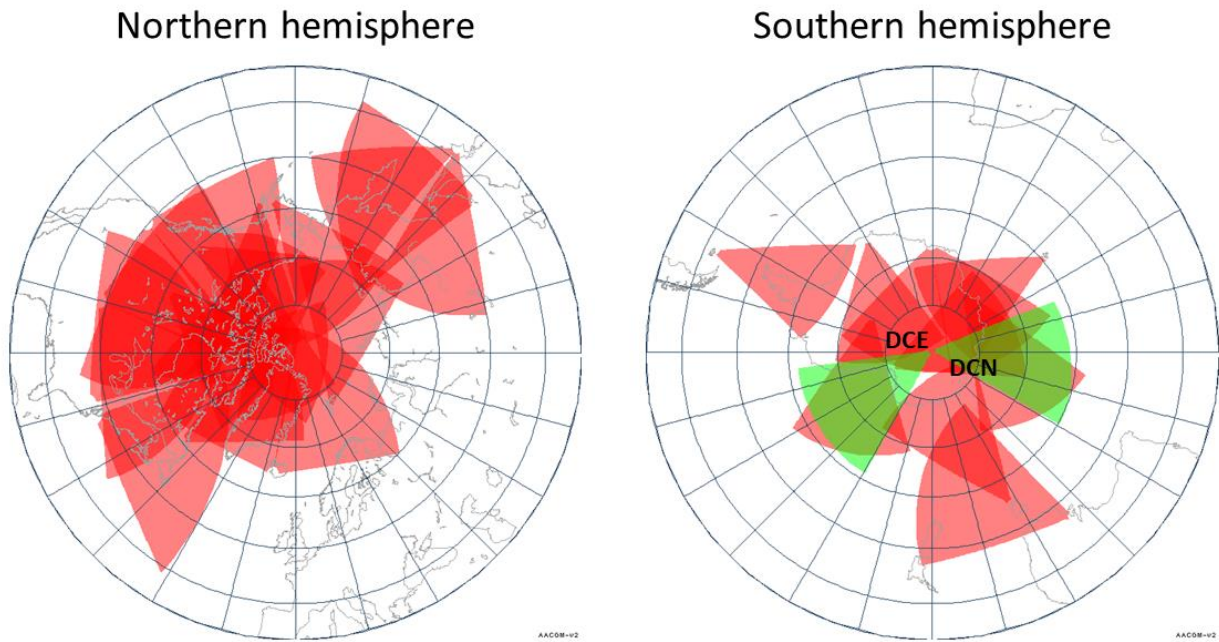


Figure 1: fields of view of SuperDARN radars currently in operations. Shaded in green, the fields of view of Dome C East (DCE) and Dome C North (DCN) radars, managed by INAF-IAPS are shown.

The snapshot of a full scan on a radar field of view is depicted in Figure 2. In this representation, positive values refer to plasma flow moving towards the radar, while negative values refer to plasma flow moving away from the radar.

All such measurements of all the radars, which all work continuously and synchronously for most of their operation time, shall then be gathered together and the ionospheric convection shall be reconstructed in near-real time over the whole polar caps in both hemispheres. The components of the plasma velocity measured along the line of sights of the radars shall be projected along the “true” directions of the velocity vectors, which lie on the isocontours of the electric potential which is established in the polar caps through the interaction of the solar wind with the Earth’s magnetosphere and ionosphere. These are the main equations which rule such system, at each given location in the ionosphere at the SuperDARN sounding altitudes:

$$\mathbf{E} = -\nabla\Phi ; \mathbf{v} = (\mathbf{E} \times \mathbf{B})/B^2, \quad (1)$$

where  $\Phi$  is the electric potential,  $\mathbf{E}$  is the electric field,  $\mathbf{B}$  is the geomagnetic field and  $\mathbf{v}$  is the convection velocity.

The original technique used to compute  $\Phi$ , only knowing the convection velocity components along the lines of sight of the single radars is fully described in [3]. The

basic idea is that the potential  $\Phi$ , as a function of co-latitude  $\theta$  and longitude  $\varphi$ , can be written as an expansion of spherical harmonic functions, whose coefficients are the actual variables to be determined:

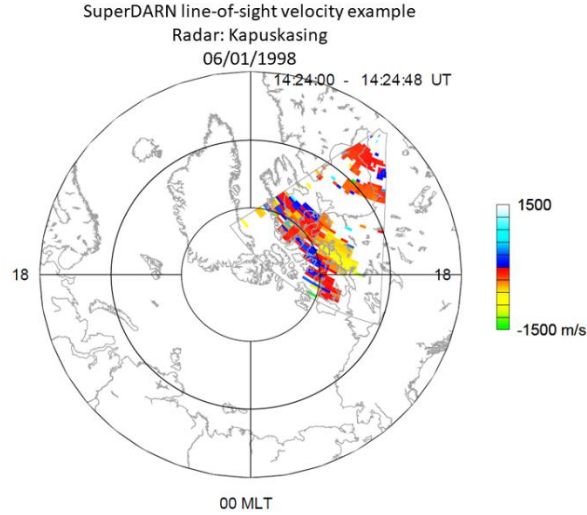


Figure 2: Example of line of sight velocities measured by a typical SuperDARN radar.

$$\Phi(\theta, \varphi) = \sum_{l=0}^L \{A_{l0} P_l^0(\cos \theta) + \sum_{m=1}^l [(A_{lm} \cos(m\varphi) + B_{lm} \sin(m\varphi)) P_m^l(\cos \theta)]\} \quad (2),$$

where  $L$  is the order of the expansion,  $P_m^l(\cos \theta)$  are the Legendre functions, and  $A_{lm}$ ,  $B_{lm}$  are the coefficients to be determined. An important thing to be considered, here, is that the expansion shall not hold on the whole co-latitude range (i.e. from  $\theta = 0$ , at the North pole, to  $\theta = 180$ , at the South pole), because there is a low latitude limit to the ionospheric convection. Therefore, the actual co-latitude is limited to a value,  $\Lambda_0$ , which constrains the convection patterns (i.e.,  $0 \leq \theta \leq \Lambda_0$  in the Northern hemisphere and  $\Lambda_0 \leq \theta \leq \pi$  for the Southern hemisphere).

For the purposes of this document, going in the deep details of  $\Phi(\theta, \varphi)$  calculation is not necessary; we just mention here the underlying procedure. After a pre-treatment, the line of sight measurements are put together for all the radars in a  $(\theta, \varphi)$  evenly binned grid ( $1^\circ$  in co-latitude, and an approximately equal width in longitude, i.e. about 110 km); as seldom happens that the coverage is uniform over the whole polar caps, model data are added in, in order to constrain the potential patterns to physical shapes and values also at those locations where no data are present. Several empirical models can be used, based on large statistics of SuperDARN data and functions of the external drivers and geomagnetic activity (e.g., interplanetary magnetic field orientation and strength, solar wind speed, Kp index...): the most recent and complete SuperDARN based convection model is the so called TS18 model [4]. Finally, equations (1) and (2) are combined, and  $A_{lm}$  and  $B_{lm}$  coefficients are evaluated through the minimization of a

$\chi^2$  function which relates the unknown “true” velocity vectors to the measured velocities.

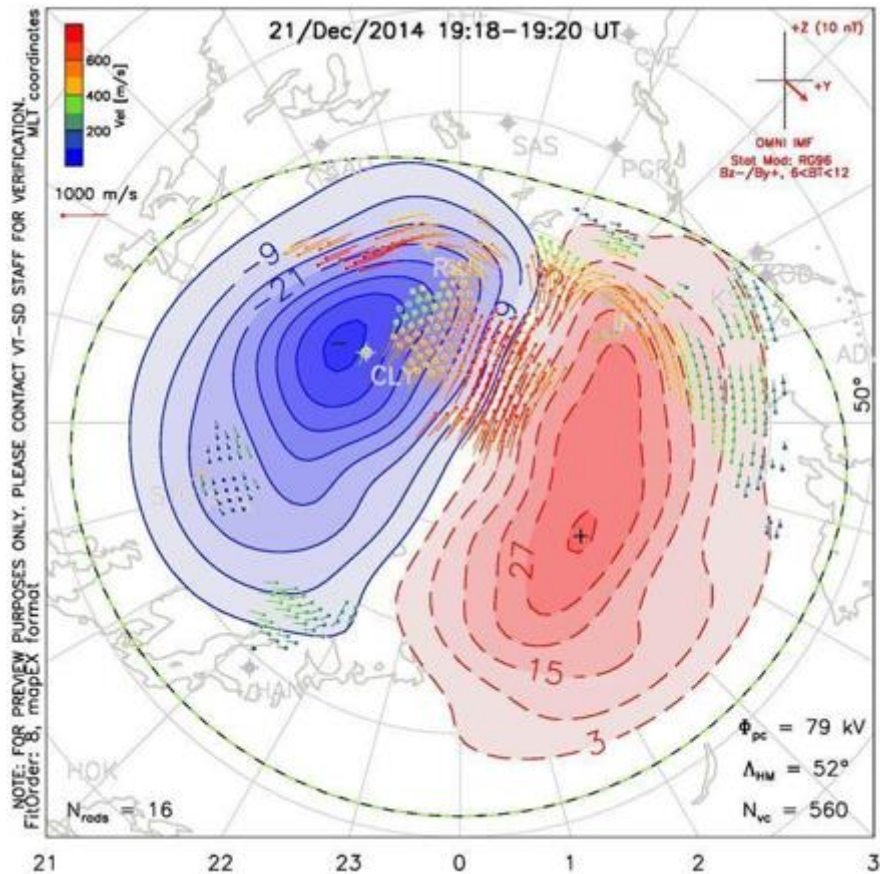


Figure 3: Example of SuperDARN convection map.

A SuperDARN convection map typically appears as in Figure 3. The coordinates used are the AACGM [5, 6] or, better, the AACGM latitude vs an AACGM local time. We will come back later on this. The isocontours of the electric potential are shown, here, in shades of red for the positive values, and in shades of blue for the negative values; in the lower left part of the figure, three important numbers are reported: 1)  $\Phi_{PC}$  is the cross-polar cap potential, i.e. the maximum potential difference in the polar cap inferred from SuperDARN measurements; 2)  $\Lambda_{HM}$  is the lower limit in latitude for the convection; 3)  $N_{vc}$  is the number of velocity vectors, i.e. of actual SuperDARN measurements, used to constrain the spherical harmonic expansion of  $\Phi$ . In the top right of the figure a small cartesian system is plotted: this represents the average strength and orientation of the Interplanetary Magnetic Field (IMF) in the GSM Y-Z plane during the 2 minutes of the scan displayed; such parameters identify the model patterns used to complete the coverage. All such information is contained in the files delivered to NODE2000.

### 3. Data format

The 8<sup>th</sup> of September 2023, 4 files in CSV format have been delivered to NODE2000, in a .zip package named “*CSV\_SuperDARN\_1410*”:

- **20150621\_20150627\_N.csv** : time series of SuperDARN parameters for the case study of the geomagnetic storm whose intensity peak occurred between 22/06/2015 and 23/06/2015. Data cover from 21/06/2015 00:02 UTC to 27/06/2015 23:58 UTC, with 2 minutes cadence. Data refers to Northern hemisphere.
- **20150621\_20150627\_S.csv** : time series of SuperDARN parameters for the case study of the geomagnetic storm whose intensity peak occurred between 22/06/2015 and 23/06/2015. Data cover from 21/06/2015 00:02 UTC to 27/06/2015 23:58 UTC, with 2 minutes cadence. Data refers to Southern hemisphere.
- **20170906\_20170911\_N.csv** : time series of SuperDARN parameters for the case study of the geomagnetic storm whose intensity peak occurred on 08/09/2017. Data cover from 06/09/2017 00:00 UTC to 11/09/2017 23:58 UTC, with 2 minutes cadence. Data refers to Northern hemisphere.
- **20170906\_20170911\_S.csv** : time series of SuperDARN parameters for the case study of the geomagnetic storm whose intensity peak occurred on 08/09/2017. Data cover from 06/09/2017 00:00 UTC to 11/09/2017 23:58 UTC, with 2 minutes cadence. Data refers to Southern hemisphere.

The first three rows of each file are fixed headers:

- *Row 1*: Fields Names;
- *Row 2*: Fields Data types (datetime, string, float, etc...);
- *Row 3*: Fields Units.

From fourth row on, data records follow. Table 1 summarizes the field content in more detail.

Field Name	Data Type	Unit	Queryable	Description
Time	datetime	UTC	Yes	Time representation ISO8601: YYYY-MO-DYTHR:MN:SC
Data points	Int	counts	Yes	Number of velocity vectors actually measured by the radars in the given time interval
Min. Lat.	Float	deg	Yes	Low latitude limit for the convection: it is the $\Lambda_0$ described in Section 2.
Geo. Lat. AACGM pole	Float	deg	No	Geographic latitude of the AACGM pole (North or South). It can be useful for coordinate transformations.
Geo. Lon. AACGM pole	Float	deg	No	Geographic longitude of the AACGM pole (North or South). It can be useful for coordinate transformations.
Geo. Rad. AACGM pole	Float	Earth radii (1 $R_E$ = 6371.2 km)	No	Distance from the centre of the Earth of the AACGM pole.
IMF B <sub>x</sub>	Float	nT	Yes	GSM* $x$ component of the interplanetary magnetic field. Data are taken from DSCOVR spacecraft, ballistically propagated to the centre of the Earth, median filtered and averaged in the 2 minutes time intervals of the radar scans. IMF is used to select the model patterns to be added to the measured vectors in order to reconstruct convection in the whole polar cap.
IMF B <sub>y</sub>	Float	nT	Yes	GSM* $y$ component of the interplanetary magnetic field.
IMF B <sub>z</sub>	Float	nT	Yes	GSM* $z$ component of the interplanetary magnetic field.
IMF B <sub>tot</sub>	Float	nT	Yes	IMF strength. $B_{tot} = \sqrt{B_x^2 + B_y^2 + B_z^2}$
Kp range	String	--	No	Range of geomagnetic Kp index during the given time interval. This parameter is used to select the model patterns to be added to the measured vectors in order to reconstruct convection in the whole polar cap. This field represents an information useful to be reported in the convection maps.

Cross-polar cap potential	Float	V	Yes	Maximum potential difference through the polar cap.
Max potential	Float	V	Yes	Maximum positive value of the electric potential.
Min potential	Float	V	Yes	Minimum negative value of the electric potential.
coef l=0	Float	V	No	$A_{00}$ coefficient of the harmonic expansion of the potential.
coef l=1, m=-1	Float	V	No	$B_{11}$ coefficient of the harmonic expansion of the potential.
coef l=1, m=0	Float	V	No	$A_{10}$ coefficient of the harmonic expansion of the potential.
coef l=1, m=1	Float	V	No	$A_{11}$ coefficient of the harmonic expansion of the potential.
...	...	...	...	Other 74 similar fields which represent the coefficients of the expansion up to order 8. Referring to Eq. 2, the coefficients with positive $m$ are the $A_{lm}$ associated to $\cos(m\varphi)$ , while the coefficients with negative $m$ are the $B_{l m }$ associated to $\sin( m \varphi)$ .

Table 1: list and description of the CSV fields.

\*GSM: Geocentric Solar Magnetospheric coordinates. With origin in the centre of the Earth, it has its X-axis from the Earth to the Sun. The Y-axis is defined to be perpendicular to the Earth's magnetic dipole so that the X-Z plane contains the dipole axis. The positive Z-axis is chosen to be in the same sense as the northern magnetic pole.

## 4. How to represent data

### 4.1 Time series data

Time series data that can be queried and simply plotted are:

- 1) The cross-polar cap potential, and the maximum and minimum potential values in the polar cap. These are the main deliverables to
- 2) NODE2000 for what concerns SuperDARN data. Their physical unit is V, but for convenience of representation, we suggest to divide them by 1000 and display them in units of kV.
- 3) Auxiliary parameters related to measurements: number of measured data and low latitude limit of the convection.
- 4) Auxiliary parameters related to model: IMF components and strength.

An example of plots of time series from the SuperDARN CSVs **20170906\_20170911\_N.csv** and **20170906\_20170911\_S.csv** is shown below (Figure

4): in the first panel IMF  $B_{tot}$ ,  $B_y$  and  $B_z$  are displayed; in the lower panel the cross-polar cap potential (CPCP) for both hemisphere is shown, in kV, along with the data points (N. measures).

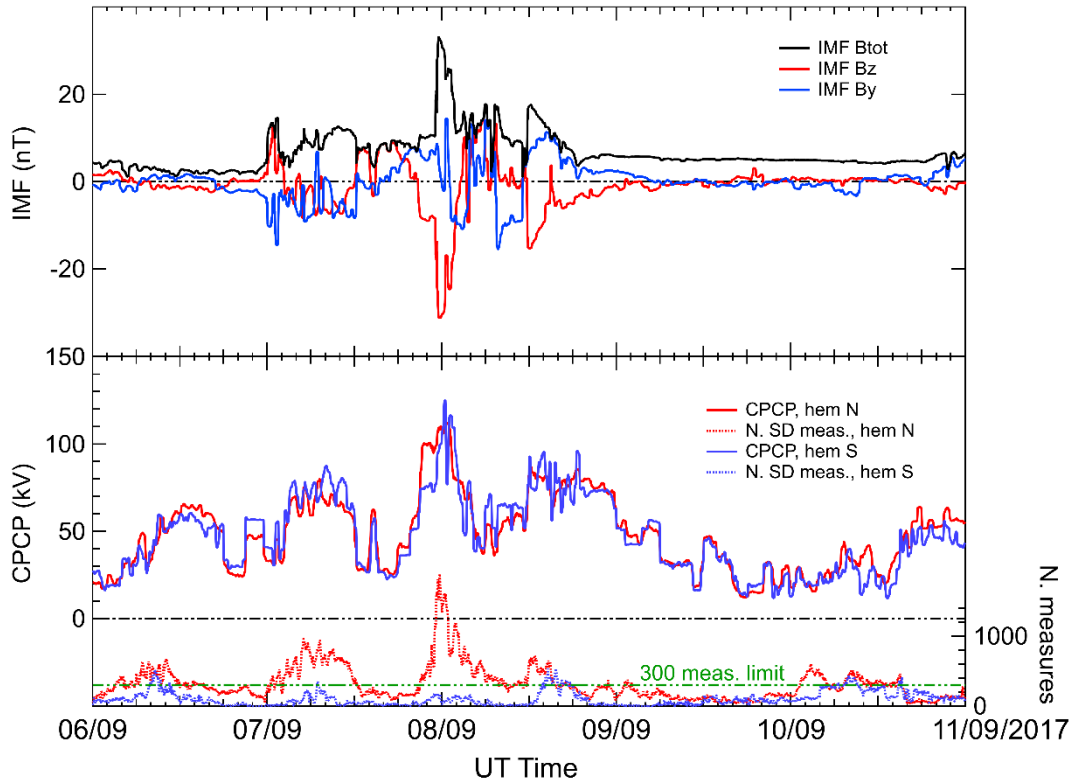


Figure 4: Example of time series extracted from SuperDARN CSVs.

## 4.2 Convection maps

The first operation to do is to calculate the electrostatic potential in the  $(\theta, \varphi)$  space, where  $\theta$  is the co-latitude in radians from 0 to  $\Lambda_0$  in the Northern hemisphere or from  $\Lambda_0$  to  $\pi$  in the Southern one, and  $\varphi$  is the longitude that ranges from 0 to  $2\pi$  radians. The procedure is the following, for each given time stamp:

- 1) Extract  $\Lambda_{\min}$  = “Lat.min.” and transform it in co-latitude in radians:  $\Lambda_0 = \pi/2 - (\pi\Lambda_{\min})/180$ .
- 2) Build a  $(\theta, \varphi)$  grid as regular as possible, i.e. a discrete set of “squares” with more or less the same extension in km for co-latitude and longitude. The SuperDARN software calculates the potential in a grid of  $1^\circ$  co-latitude (approximately 111 km) and an equal spacing in longitude. For each co-latitude,  $\theta$ , the number of grid cells in longitude are determined by:  $n(\theta) = \text{NINT}(360 * \sin(\theta))$ , where NINT

is the “nearest-integer” function. Ex: for  $\theta = 10^\circ$  co-lat (equivalent to  $80^\circ$  lat),  $n(\theta) = 63$  equally spaced intervals in longitude,  $[0^\circ, (360/63)^\circ]$ ,  $[(360/63)^\circ, 2 \times (360/63)^\circ]$ , ...,  $[62 \times (360/63)^\circ, 63 \times (360/63)^\circ]$ , and the longitude value to be used is the one at the centre of each interval, of course transformed in radians. This is the grid of points that the SuperDARN software uses for computing the coefficients of the spherical harmonic expansion of the electrostatic potential starting from measurements and model data. But as we already have the coefficients and we only want to calculate the potential on a grid, the binning of the grid could also be thicker, provided  $0 < \theta \leq \Lambda_0$ , for North, or  $\Lambda_0 \leq \theta < \pi$  for South.

- 3) Read the coefficients fields and organize them so that to group the  $A_{l0}$  ( $0 \leq l \leq 8$ ) together (Fields of the kind “Coef l=0”, “Coef l=1”, “Coef l=2”, etc...), and, for each  $l > 0$ , distinguish the  $A_{lm}$  (Fields of the kind “Coef l=1, m=1”, “Coef l=2, m=1”, “Coef l=2, m=2”, etc...), from the  $B_{lm}$  (Fields of the kind “Coef l=1, m=-1”, “Coef l=2, m=-2”, “Coef l=2, m=-1”, etc...) coefficients.
- 4) Apply eq. 2 to each point of the  $(\theta, \varphi)$  grid, using the Legendre functions that should be already available in whatever programming language.

Once the potential is computed, it shall be represented on a polar map, in terms of isocontours. In principle, the calculation done is independent of the coordinate system used, provided it is a spherical coordinate system (with fixed  $R=6771.2$  km from the centre of the Earth, i.e. about 400 km above the surface). The minimum latitude that can be set for the map should be a bit southward (northward, for the Southern hemisphere) of the minimum latitude to which convection is constrained in the entire dataset; a safe value can be  $\pm 30^\circ$ . As a first attempt, contours can be plotted in geographic coordinates, as shown in the example below (Figure 5).

Some basic information that should be present in the map: 1) the value of the cross-polar cap potential for the given interval (108 kV, in this case); 2) the vector representation of the IMF in the GSM ( $y, z$ ) plane (it can be seen in the top right of the figure), along with the value of  $B_{tot}$  (24 nT in this example); 3) the mention to the model used (TS18-Kp MODEL); 4) the Kp range taken into account by the model for the given interval (“Kp range” field of the CSV files), “ $6 < Kp < 8$ ” in this example.

08 Sep 2017

108 kV

01:00:00 - 01:02:00 UT

24 nT  
(-00 min)

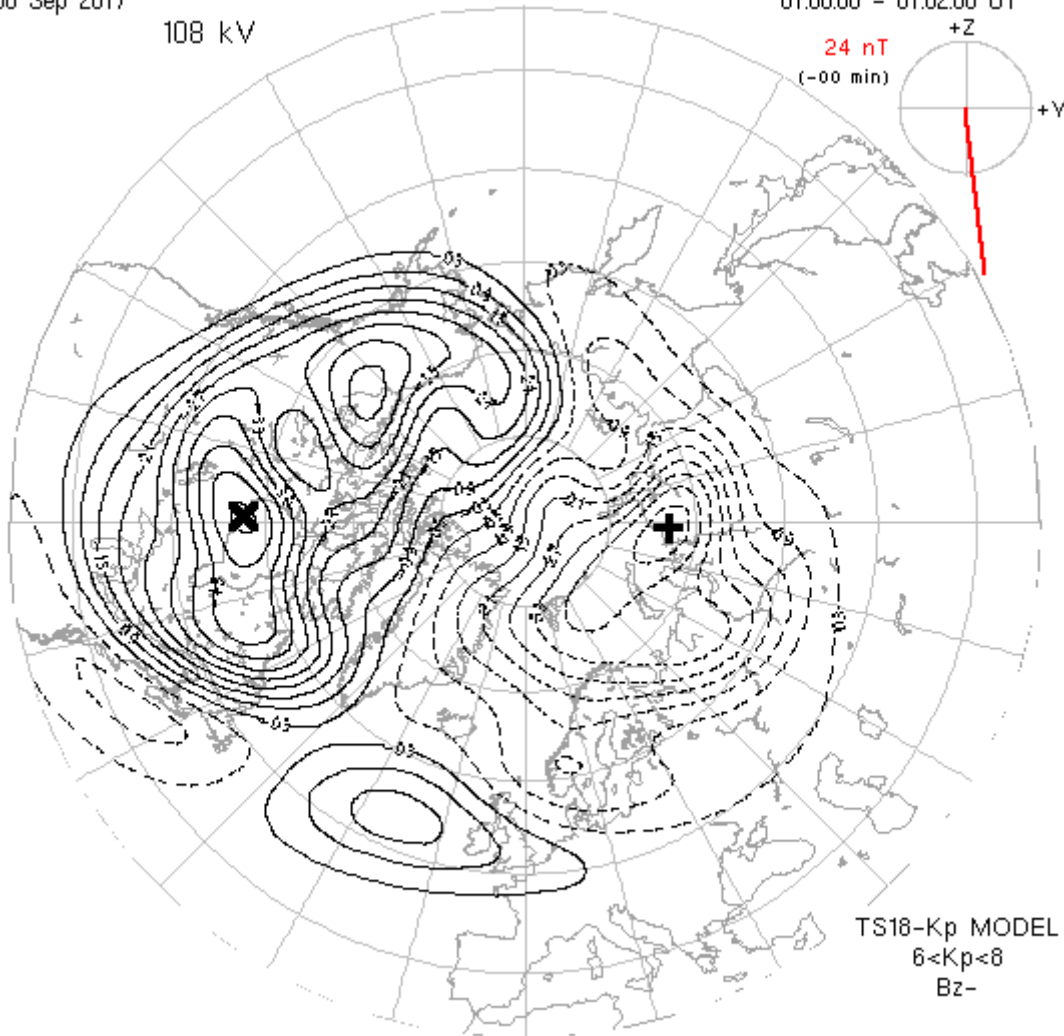
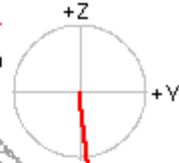


Figure 5: example of SuperDARN convection map in geographic coordinates.

## 5. Representation in AACGM coordinates

As previously mentioned, the preferred representation for SuperDARN maps utilizes the AACGM coordinate system [5, 6]. The motivation for introducing this system arose from the need of comparing ground-based radar backscatter measurements from locations in both hemispheres. The AACGM coordinates of a given point, specified by its geographic latitude, longitude and altitude above the surface of the Earth, are determined by following the magnetic field line from the geographic starting point to the magnetic dipole equator. The AACGM coordinates are then given by the latitude and longitude of the dipole field line that connects the point on the magnetic equator to the surface of the Earth.

The conversion from geographic coordinates is not trivial, it requires a spherical harmonic expansion of the dipole field, with a related set of coefficients to be applied.

Conversion software, both in IDL and C, can be downloaded here: <https://superdarn.thayer.dartmouth.edu/aacgm.html>, along with the most up-to-date set of coefficients.

For example, in Figure 6, the same map of Figure 5 is shown but in AACGM coordinates.

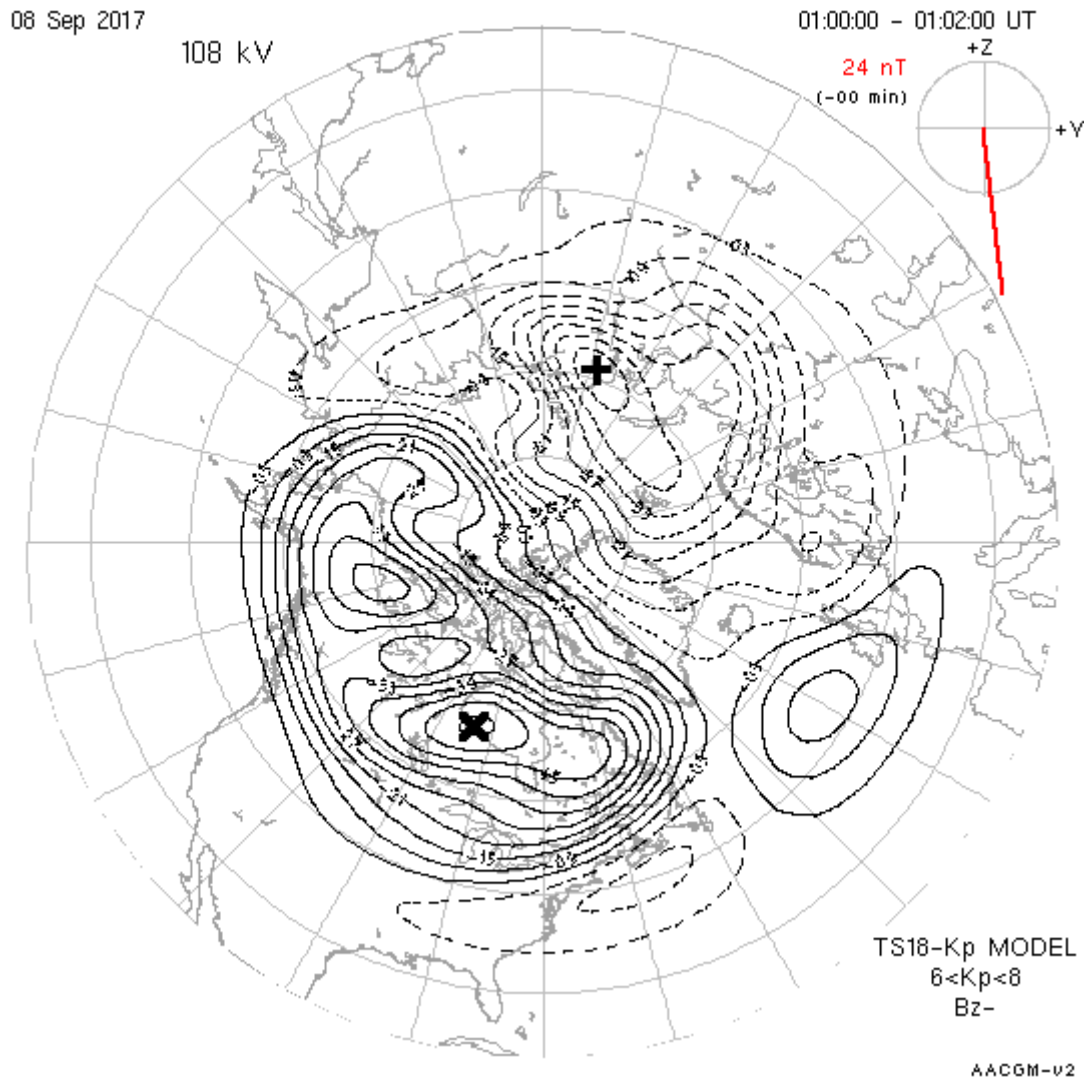


Figure 6: Example of SuperDARN convection map in AACGM coordinates.

Another representation very often used, it is made by replacing the AACGM longitude with the AACGM local time:

$$\text{AACGM\_LT} = \text{UTC} + \text{AACGM\_long}/15 \quad (3)$$

If  $\text{AACGM\_LT} > 24$ ,  $\text{AACGM\_LT} = 24 - \text{AACGM\_LT}$ . This representation is useful in a polar map like those shown above, as it is very easy to catch the convection symmetries with respect to the illumination conditions. An example of such a representation is given in Figure 7, usually with local noon on top.

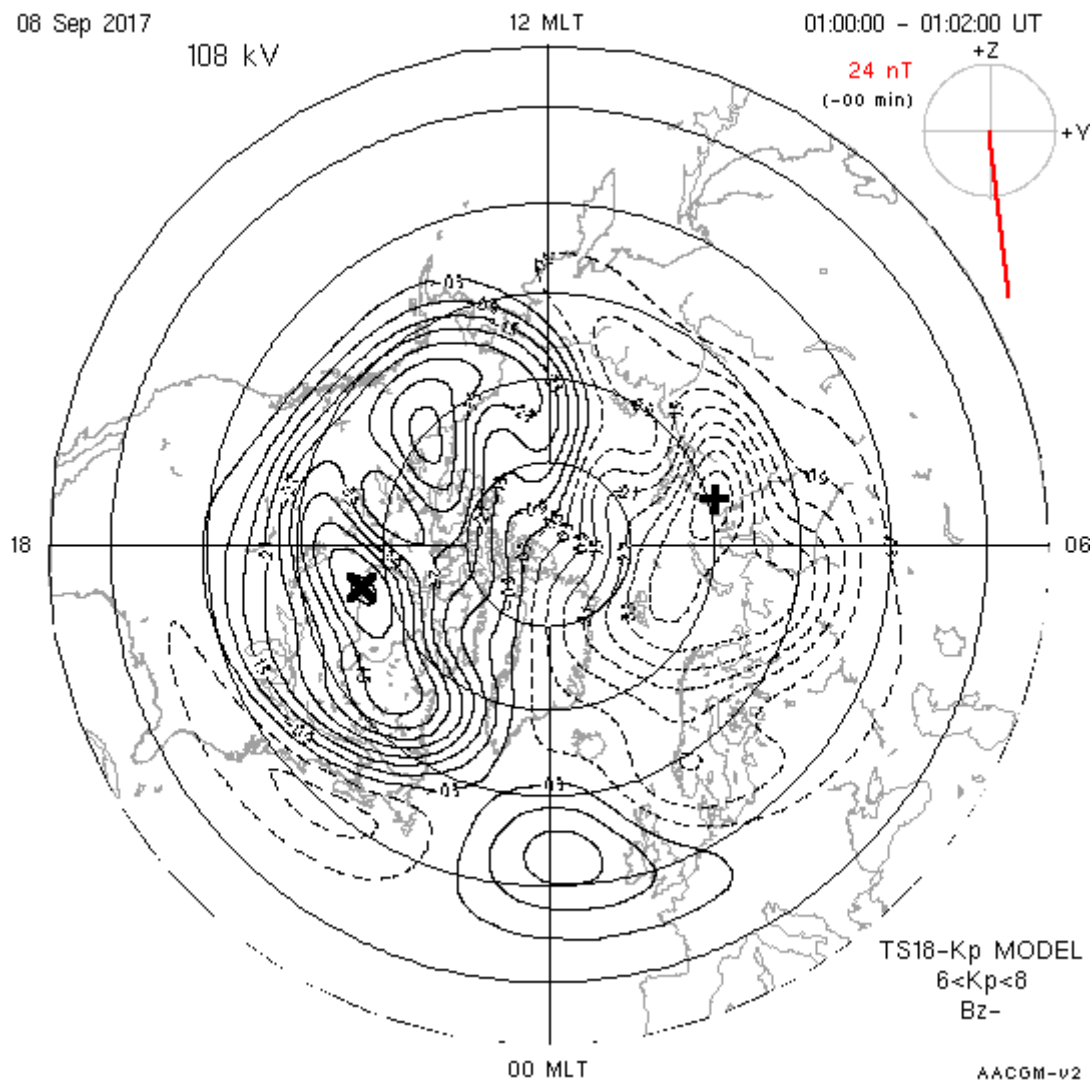


Figure 7: Example of SuperDARN convection map in AACGM latitude and local time.

## 6. References

- [1] SuperDARN Data Analysis Working Group, Thomas, E. G., Reimer, A. S., Bland, E. C., Burrell, A. G., Grocott, A., Ponomarenko, P. V., Schmidt, M. T., Shepherd, S. G., Sterne, K. T., and Walach, M.-T, SuperDARN Radar Software Toolkit (RST) 5.0 (v5.0). Zenodo (2022). <https://doi.org/10.5281/zenodo.7467337>
- [2] Greenwald, R.A., Baker, K.B., Dudeney, J.R. *et al.*, DARN/SuperDARN, A global view of the dynamics of high-latitude convection, *Space Sci Rev*, **71**, 761–796 (1995). <https://doi.org/10.1007/BF00751350>
- [3] Ruohoniemi, J.M., and K.B. Baker, Large-scale imaging of high-latitude convection with Super Dual Auroral Radar Network HF radar observations, *J.*

*Geophys. Res., Space Physics*, **103**, 20797-20811 (1998).  
<https://doi.org/10.1029/98JA01288>

[4] Thomas, E. G., and S. G. Shepherd, Statistical Patterns of Ionospheric Convection Derived From Mid-latitude, High-Latitude, and Polar SuperDARN HF Radar Observations, *J. Geophys. Res., Space Physics*, **123(4)**, 3196-3216 (2018).  
<https://doi.org/10.1002/2018JA025280>

[5] Baker, K. B., and S. Wing, A new coordinate system for conjugate studies at high latitudes, *J. Geophys. Res.*, **94(A7)**, 9139 (1989).  
<https://doi.org/10.1029/JA094iA07p09139>

[6] Shepherd, S. G., Altitude-Adjusted Corrected Geomagnetic Coordinates: Definition and Functional Approximations, *J. Geophys. Res., Space Physics*, **119(9)**, 7501-7521 (2014). <https://doi.org/10.1002/2014JA020264>